



# Comparative Analysis of Eccentric Glenosphere in Reverse Total Shoulder Arthroplasty: A Computer Simulation Study

Xiaopei Xu, Qingnan Sun, Yang Liu, Dong Wang , Shuo Diao, Hanzhou Wang, Yuling Gao, Tianchao Lu, Junlin Zhou 

Department of Orthopedic Surgery, Beijing Chaoyang Hospital, Capital Medical University, Beijing, 100020, People's Republic of China

Correspondence: Junlin Zhou, Department of Orthopedic Surgery, Beijing Chaoyang Hospital, Capital Medical University, 8 Gongren Tiyuchang Nanlu, Chaoyang District, Beijing, 100020, People's Republic of China, Tel/Fax +86-01085231227, Email junlinzhou\_article@outlook.com

**Objective:** The aim was to evaluate the effects of different glenosphere eccentricities on impingement, range of motion (ROM), and muscle length during standard activities in reverse total shoulder arthroplasty (RSA).

**Methods:** In this study, we utilized computational modeling techniques to create native shoulder and shoulder models undergoing RSA and simulate shoulder movements in all abduction-adduction, flexion-extension, and rotation. We tested a total of 36 different glenosphere configurations, which included three different inferior tilts (0°, +10°, +20°) and two different lateral offsets (0 mm and +4 mm), as well as six different glenosphere eccentricities (concentricity, inferior, posterior, anterior, anteroinferior, and posteroinferior). We evaluated the maximum impingement-free ROM, impingement sites, and muscle lengths.

**Results:** All glenosphere configurations exceeded 50% of native shoulder ROM in three planes and total global ROM. In abduction-adduction, there was no significant difference among the different glenosphere eccentricities ( $p > 0.05$ ). In flexion-extension, the posteroinferior eccentricity had the maximum ROM among the different eccentricities, but no significant difference among the different glenosphere eccentricities ( $p > 0.05$ ). In rotation, there was a significant difference overall, and anteroinferior eccentricity had a significant advantage over concentricity ( $p < 0.05$ ). In total global ROM, anteroinferior eccentricity had a significant advantage over concentricity when lateral offset was 0 mm ( $p < 0.05$ ). In all models of glenosphere eccentricities, only the elongation of the infraspinatus muscle was statistically significant ( $p < 0.05$ ).

**Conclusion:** Glenosphere eccentricity significantly influenced rotation, total global ROM, and the length of the subscapularis muscle. Among them, anteroinferior offset achieved the maximum ROM in abduction-adduction, rotation, and total global activities. Both anteroinferior and inferior glenoid eccentricity showed significant advantages over the concentricity in rotation and total global ROM.

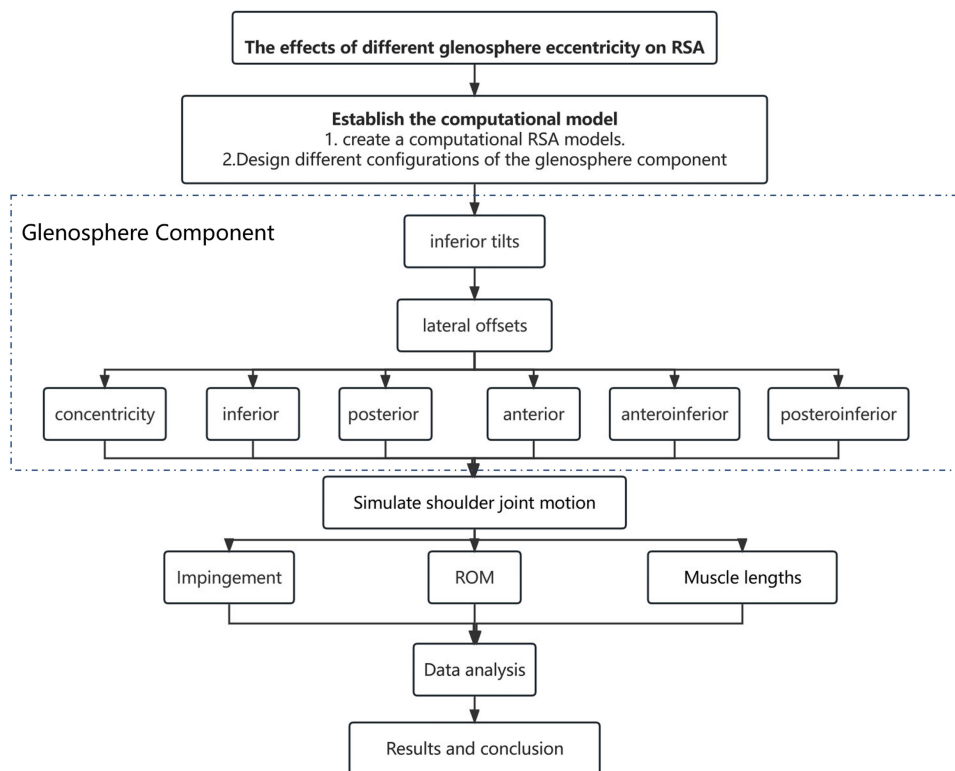
**Level of Evidence:** Basic Science Study; Computer Modeling.

**Keywords:** reverse shoulder arthroplasty, glenosphere eccentricities, impingement, notching, range of motion, muscle length

## Introduction

Reverse total shoulder arthroplasty (RSA) has emerged as a widely accepted approach for managing shoulder pathologies, including Neer's 3 and 4-part proximal humerus fractures, cuff tear arthropathy, revision arthroplasty, and degenerative diseases.<sup>1-4</sup> Since 2014, the annual number of RSA surgeries performed in the United States has surpassed anatomical total shoulder arthroplasty (TSA), with an estimated 80,000 procedures performed each year.<sup>5</sup> With the increasing popularity of RSA, there has been a growing understanding of its associated complications. During the mid- to long-term follow-up after RSA surgery, the incidence of impingement and notching has been reported to range from 9.6% to 68%.<sup>6,7</sup> The mechanism of scapular notching remains incompletely understood, but it is primarily attributed to mechanical contact between the polyethylene implant component and the scapular border during arm movements, including abduction, adduction, extension, internal and external rotation (IR and ER).<sup>7,8</sup> This contact leads to wear of the polyethylene material, chronic inflammation, and localized osteolysis.<sup>9</sup>

**Graphical Abstract**



The design of the implant and the method of surgery can significantly affect the results, as can the characteristics of the glenoid and humerus. Indeed, these factors can directly alter the stability of the implant internally, the forces exerted by muscles, range of motion (ROM), impingement, and notching. Some studies have indicated that glenosphere offset can have an impact on the ROM. Inferiorization and lateralization of the glenosphere’s position have been shown to reduce the risk of impingement and notching and improve shoulder mobility.<sup>10-14</sup> There have been computer studies conducted to evaluate the comparisons in ROM for different glenosphere eccentricities. These studies have explored various eccentricities such as central, inferior, posteroinferior eccentricity, and<sup>13</sup> inferior and anterior eccentricity,<sup>15</sup> as well as superior and inferior eccentricity.<sup>16</sup> However, to the best of our knowledge, there is currently no comprehensive research evaluating the effects of different glenosphere eccentricities on shoulder joint mobility, impact risk, and muscle length.

To fill this knowledge gap and to make standardized comparisons, we conducted a computational simulation study. Due to the limited research on the eccentricity position of the glenosphere, we hypothesize that there are other directions of hypothesis that may achieve a larger impingement-free ROM of the shoulder joint. This study aims to provide evidence-based recommendations for glenosphere eccentricity in RSA, ultimately improving patient outcomes and surgical decision-making.

**Materials and Methods**

**Shoulder Computed Tomography Data and Computational Model**

This basic science study used three-dimensional (3D) reconstructed computational models based on computed tomography (CT). We retrospectively collected data from consecutive patients diagnosed with primary osteoarthritis or cuff tear arthropathy in the orthopedic department of Beijing Chaoyang Hospital from January 2022 to February 2022. Exclusion criteria were age less than 18 years. Patients with significant bony dysplasia of the scapula, glenoid, or humerus or with a previous injury. Their radiological information was collected. This is in keeping with existing

literature in this area,<sup>17–21</sup> which used normal shoulder CT scans. We obtained ethical approval prospectively. Finally, six patients (4 women and 2 men) were included in the current study, with an average age of 72.4 years. Bone tissue was manually segmented from other tissues by automatic grayscale threshold segmentation (minimum 200 Hounsfield units) in Mimics software (Materialise, Leuven, Belgium), and the bone geometric boundaries were constructed.<sup>22</sup> 3D bone geometry was reconstructed using Geomagic Wrap (3D Systems, Rock Hill, USA) and overlaid with the original CT images to assess the accuracy of the reconstruction. The reconstructed model was subsequently brought into SolidWorks 2018 (Dassault Systèmes Corp., Concord, MA, USA) for further modeling. All standard axes and planes of the bone structure were defined according to the standards of the International Society of Biomechanics (ISB).<sup>23</sup> To standardize the position of the humerus and scapula for all patients, the glenoid version and inclination were corrected individually in each case aiming to be neutral or the closest to neutral.<sup>24,25</sup>

## Computational Simulation of RSA

The Comprehensive<sup>®</sup> Reverse Shoulder System (Biomet, Inc., Warsaw, IN, USA) was used in this study. The simulation of the surgery mainly includes three steps: implantation of the humeral prosthesis implantation, glenoid prosthesis implantation, and assembly of the two components. Using Solidworks 2018 to simulate RSA, visualization can be performed from the coronal, sagittal, and transverse planes, respectively. Surgeons were trained and practiced with the software and simulated reverse shoulder arthroplasty according to standard techniques<sup>26,27</sup> under the supervision of two experienced shoulder surgeons. The scapula model was modified to be as close as possible to the neutral version and inclination. This included a glenosphere with a diameter of 36 mm, which was the best fit in all instances, and a standard glenoid baseplate with a diameter of 28 mm and a central peg of 15 mm. The central peg's entry point was centered in the width of the glenoid and at a height that made the baseplate level with the lower rim of the glenoid. We tested 36 different glenoid configurations combining 3 different inferior tilts (0°, +10°, +20°), 2 different lateral offsets (+0 mm and +4 mm), and 6 different glenosphere eccentricities (+0 mm, +2 mm inferior, +2 mm posterior, +2 mm anterior, +2 mm anteroinferior, and +2 mm posteroinferior). The lateral offset of 4 mm is lateralized by the lateralized glenosphere<sup>28</sup> (see Figure 1).

On the humeral side, all models used a humeral osteotomy at a retrotorsion tangle of 20° relative to the intercondylar axis.<sup>26,27</sup> An Onlay humeral prosthesis with a 147° neck-shaft angle is implanted, consistently positioned at the level of the greater tuberosity. The implanted humeral metal stem has a 135° inclination angle, and the polyethylene cup has a 12° angle. Using tangent matching under functional conditions, the glenohumeral joint of the RSA was modeled as a center-rotating ball-and-socket joint.

## Simulating Kinematic and Impingement

The native shoulder and each of the 36 combinations were exported as.stl files from SolidWorks for the humeral side and scapular side, respectively, and then imported into Blender 3.0 (Blender Foundation, Amsterdam, the Netherlands) for the evaluation of the impingement-free ROM. The ROM was evaluated by simulating standard kinematics: abduction-adduction (parallel to the coronal plane), flexion-extension (parallel to the sagittal plane), and internal-external rotation. Global ROM is defined as the sum of all 6 motions. The evaluation of abduction-adduction and flexion-extension was conducted with the arm positioned in a neutral rotation. IR and ER were measured with the arm positioned in 10° abduction relative to the sagittal plane.

Assuming that the polyethylene cup and the glenosphere are in perfect contact and completely match during movement the 3D geometries of the scapula, humerus, and prosthesis were discretized into a mesh with a maximum pixel size of 1 mm<sup>2</sup>. Any impingement or overlap of voxel graphics was utilized for detecting impingements between bone-to-bone and bone-to-implant interactions. When an impingement was detected during motion, the software system recorded the positions of the overlapping voxels and the angle of rotation. The measurements were performed by one observer with a resolution of 0.1° (see Figure 2).

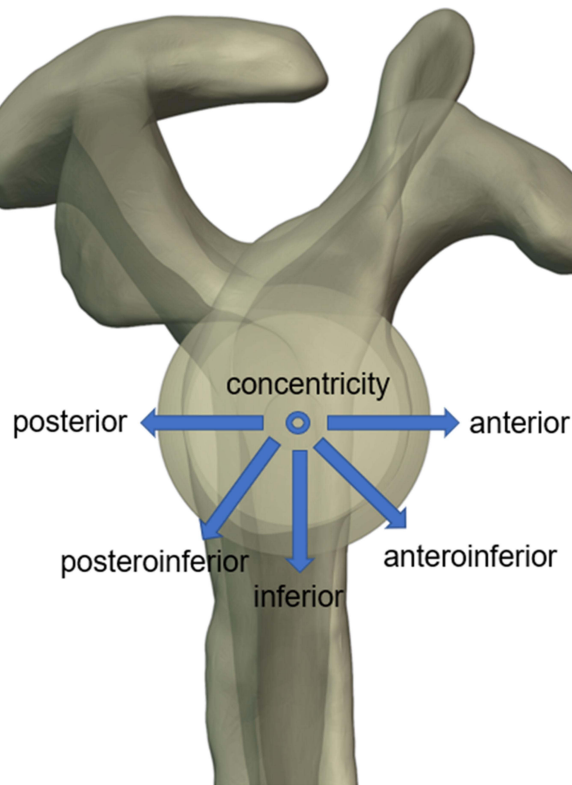


**Figure 1** This figure shows 6 different glenosphere eccentricities positions (concentricity, +2 mm inferior, +2 mm posterior, +2 mm anterior, +2 mm anteroinferior, and +2 mm posteroinferior) with no change in the baseplate.

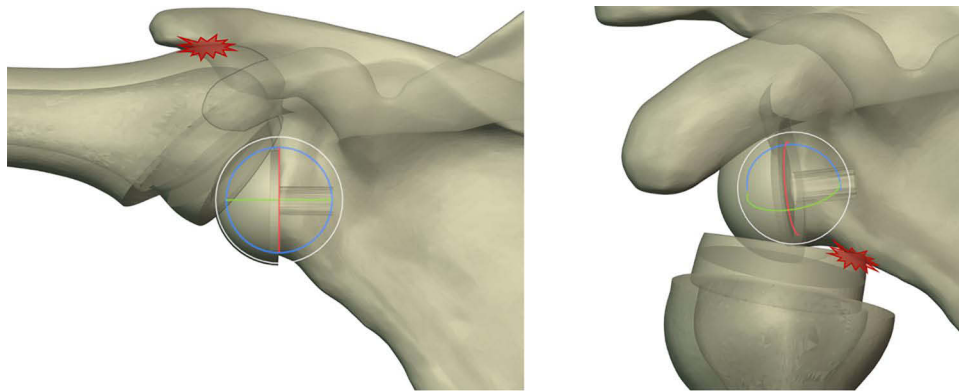


**Figure 2** Shows the simulation of impingement in the shoulder joint after RSA during abduction and internal rotation.

### Muscle Length

The length of the muscle was determined in a neutral position in relation to the humerus. The variation in the length of the rotator cuff muscles was approximated by comparing the line segments that represented these muscles. Due to the wide range of muscle attachments, for the standardization and simplification of measurement, we have uniformly defined the pseudo-origins and insertions of each deltoid muscle and rotator cuff. The pseudo-origins of the anterior, middle, and posterior bundles of the deltoid muscle are, respectively, at the lateral third of the clavicle, the lateral acromion, and the most lateral scapular spine. The insertion point for all three bundles is the deltoid tuberosity of the humerus. The pseudo-origin of the supraspinatus was identified as the supraglenoid tubercle, while its insertion point was determined to be the upper edge of the greater tuberosity. The pseudo-origins of the infraspinatus and subscapularis muscles were established

at their furthest lateral bone attachment on the scapula, and their insertion points were located at the center of the greater and lesser tubercles, respectively. In addition, we measured the superior, middle, and inferior bundles of the infraspinatus and teres minor muscles separately and then took the average as the length of the muscle. The average length of each muscle at each degree of movement was evaluated as a percentage of the corresponding muscle length in the original shoulder. To be specific, a positive percentage signifies that the muscle has lengthened compared to the normal shoulder, while a negative percentage signifies that the muscle has shortened compared to the original shoulder.

## Statistical Analysis

Statistical analysis was performed using IBM SPSS 26 (IBM, Armonk, New York, USA) and Origin 2021 (Origin Lab, New York, USA). Data analysis includes descriptive statistics, such as mean, standard deviation (SD), and 95% confidence interval (CI), which apply to all ROM and muscle elongation measurements. We compared ROM and muscle elongation using a one-way analysis of variance (ANOVA), and Tukey HSD post hoc test was used for analysis and paired sample *t*-test. A statistically significant difference was considered when  $P < 0.05$ .

## Results

### Influence of Eccentric Glenosphere on ROM

Overall, the glenosphere offset has a significant impact on rotation and global ROM. Anteroinferior and inferior offset have a significant advantage in terms of total rotation and global ROM compared to the center. Complete tables and graphs, which present all ROMs for every configuration, can be found in the [Supplementary Material](#). The most crucial observations are outlined below, categorized by the plane of motion.

#### Abduction-Adduction

Among the 36 combinations, none of them exceeded the native ROM of 109.1° for abduction-adduction, even though all combinations achieved at least 50% of the native ROM (see [Figure 3](#)). In this plane of motion, there were no statistically

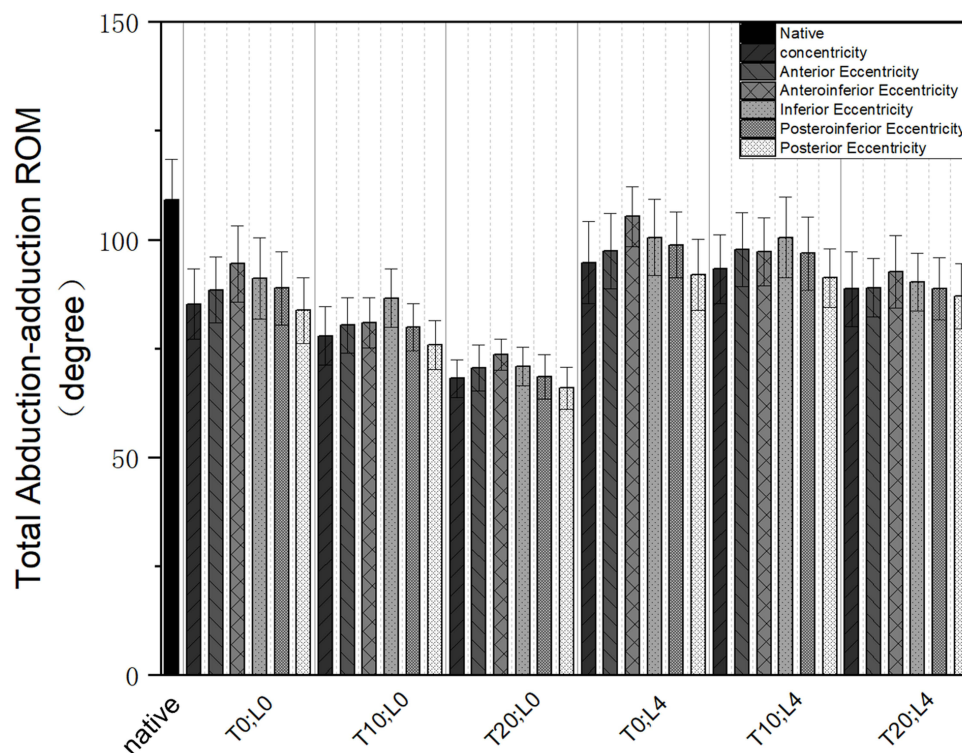


**Figure 3** Shows the comparison of the abduction-adduction ROM for different glenosphere eccentricities under all glenoid options. Native: the native shoulder, T: tilt, and L: lateral offset.

significant differences in glenosphere eccentricity between different positions ( $p > 0.05$ ). However, for tilt angles of  $0^\circ$  and  $20^\circ$ , the anteroinferior eccentricity had the maximum ROM compared to other eccentricities, although the differences were not significant ( $p > 0.05$ ). Among these glenoid options, the maximum ROM was observed at  $105.3^\circ$  for the tilt angle of  $0^\circ$  and lateral offset of 4 mm (T0L4). In adduction motion, the anteroinferior eccentricity had the largest ROM among eccentricities. For abduction motion, the anteroinferior eccentricity achieved the maximum ROM for both tilt angles of  $0^\circ$  and  $20^\circ$  and has a significant advantage compared to all other glenosphere offsets ( $p < 0.05$ ).

### Flexion-Extension

Among the 36 combinations, none of them exceeded the native ROM of  $283^\circ$ . In all glenoid options, the posteroinferior eccentricity had the maximum ROM compared to other eccentricities in the plane of motion (see Figure 4). Furthermore, in the T10L4 and T20L4, the posteroinferior eccentricity demonstrated a significant advantage over the anteroinferior eccentricity ( $p < 0.05$ ). Furthermore, in the flexion, the posteroinferior eccentricity had the maximum ROM, which was significantly better than the center, anterior, and anteroinferior ( $p < 0.05$ ), while in extension, there were no statistically significant differences in glenosphere offset ( $p > 0.05$ ).

### Internal-External Rotation

All measurements of rotation were performed at a position of  $10^\circ$  of shoulder abduction. Similarly, among the 36 combinations, none of them exceeded the native ROM of  $174^\circ$ . In all glenoid options, significant differences were observed among all glenosphere eccentricities (see Figure 5). Specifically, anteroinferior eccentricity exhibited a significant advantage over concentricity posterior and anterior offset ( $p < 0.05$ ), while no significant differences were found between anteroinferior, inferior, and posteroinferior eccentricities ( $p > 0.05$ ). The maximum ROM observed in the anteroinferior eccentricity was  $164.5$  degrees for the T10L4. Additionally, in IR, anteroinferior eccentricity had the maximum ROM among all different glenosphere eccentricities and showed a significant advantage over concentricity and posteroinferior eccentricity ( $p < 0.05$ ). In ER, posteroinferior eccentricity had the maximum ROM and demonstrated a significant advantage over concentricity and anterior eccentricity ( $p < 0.05$ ).

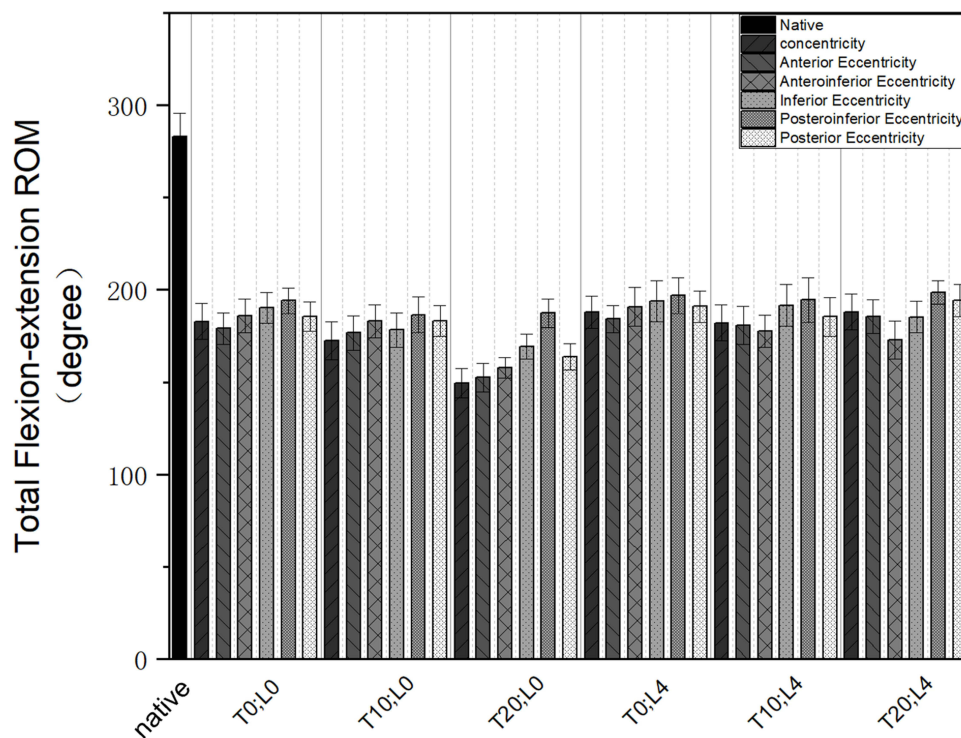
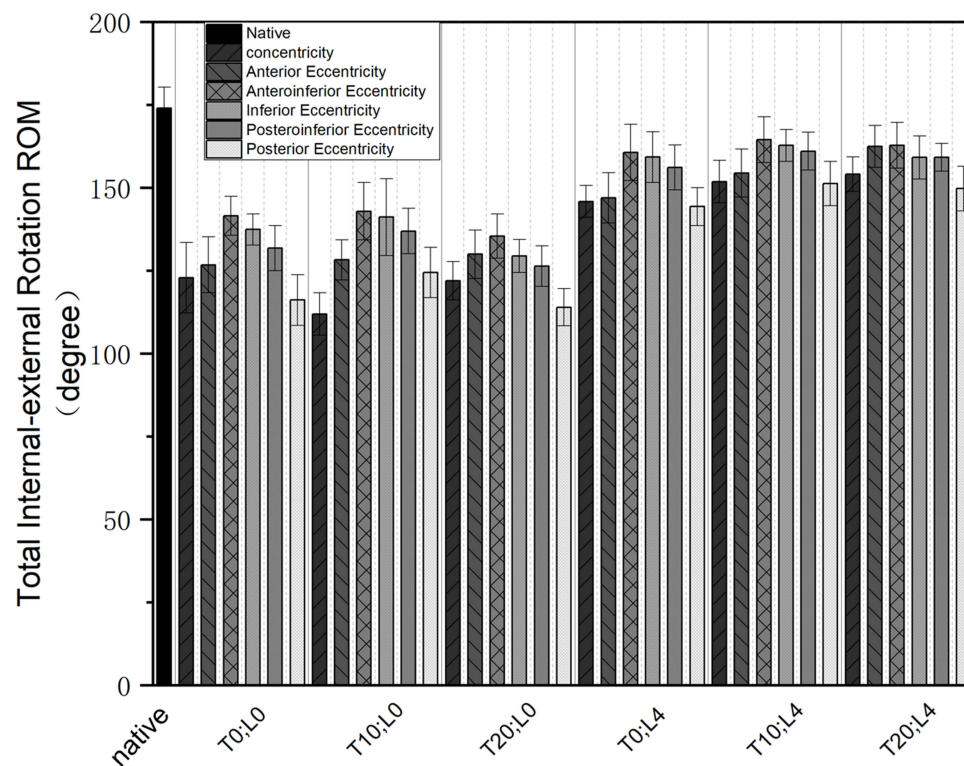


Figure 4 Shows the comparison of the flexion-extension ROM for different glenosphere eccentricities under all glenoid options. Native: the native shoulder, T: tilt, and L: lateral offset.



**Figure 5** Shows the comparison of the internal-external rotation ROM for different glenosphere eccentricities under all glenoid options. Native: the native shoulder, T: tilt, and L: lateral offset.

### Total Global ROM

In this assessment of ROM, none of the combinations exceeded the native ROM of 566.1°. In all glenoid options, there were significant differences among different glenosphere eccentricities (see [Figure 6](#)). Specifically, in the case of 0mm lateral offset, anteroinferior eccentricity demonstrated a significant advantage over the concentricity position ( $p < 0.05$ ), while no significant differences were found among anteroinferior, inferior, and posteroinferior eccentricities ( $p > 0.05$ ). Among these combinations, the T0L4 combination had the largest ROM for anteroinferior eccentricity, reaching up to 456.7°.

### Sites and Frequency of Impingement

In general, the sites and frequencies of impingement during shoulder joint movements vary for different glenoid characteristics. [Figure 7](#) presents a heatmap of the frequency of impingement sites for 6 different glenosphere eccentricities under different motions. During abduction, the most common impingement occurs between bone structures, primarily involving the impingement of the humeral greater tuberosity and the acromion. Additionally, impingement can occur between bone and prosthesis, such as the impingement between the glenoid and the poly (commonly observed in anteroinferior and inferior eccentricities). During extension, the displacement of the glenosphere significantly affects the impingement sites.

Furthermore, impingement sites are relatively consistent during adduction, flexion, and rotation, including impingement between the neck of the scapula and the poly, the lesser tuberosity and the coracoid process, as well as anterior and posterior impingements of the glenoid-neck with the poly, respectively. [Table 1](#) illustrates impingement sites for different glenoid options when the glenosphere anteroinferior eccentricity.

### Muscle Length

In all combinations of glenosphere eccentricities, lengthening of the deltoid and infraspinatus muscles was observed, whereas the teres minor was shortened relatively to the native, and the subscapularis was lengthened in partial combinations. There were significant differences in the changes of subscapularis muscle between the whole group ( $p < 0.05$ ), and there were significant differences between the anteroinferior and the concentric and posterior eccentricity ( $p$

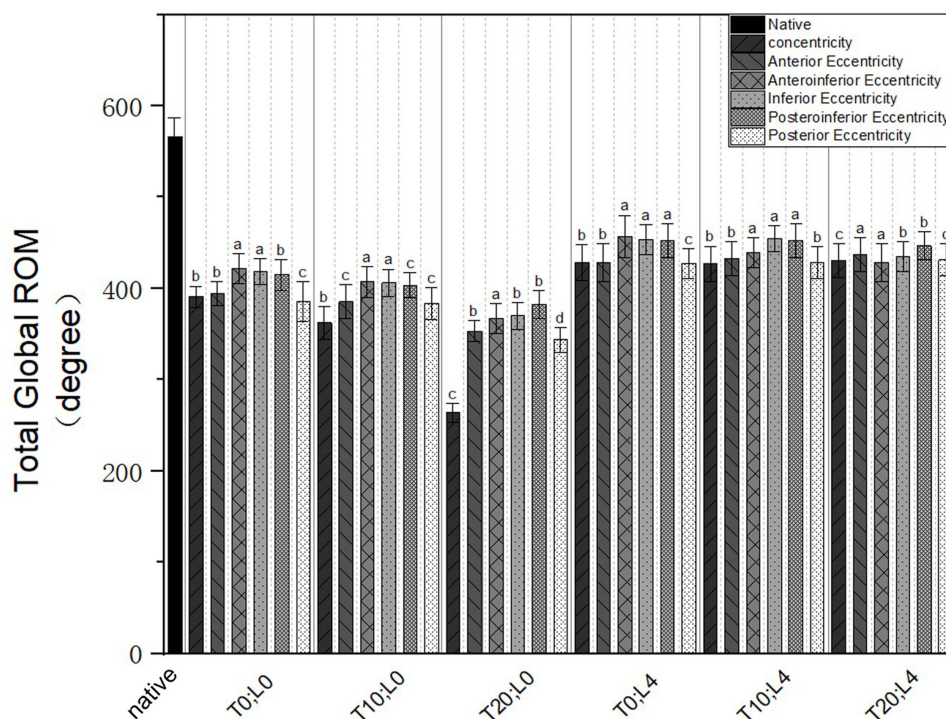


Figure 6 Shows the comparison of the Total global ROM for different glenosphere eccentricities under all glenoid options. Native: the native shoulder, T: tilt, and L: lateral offset.

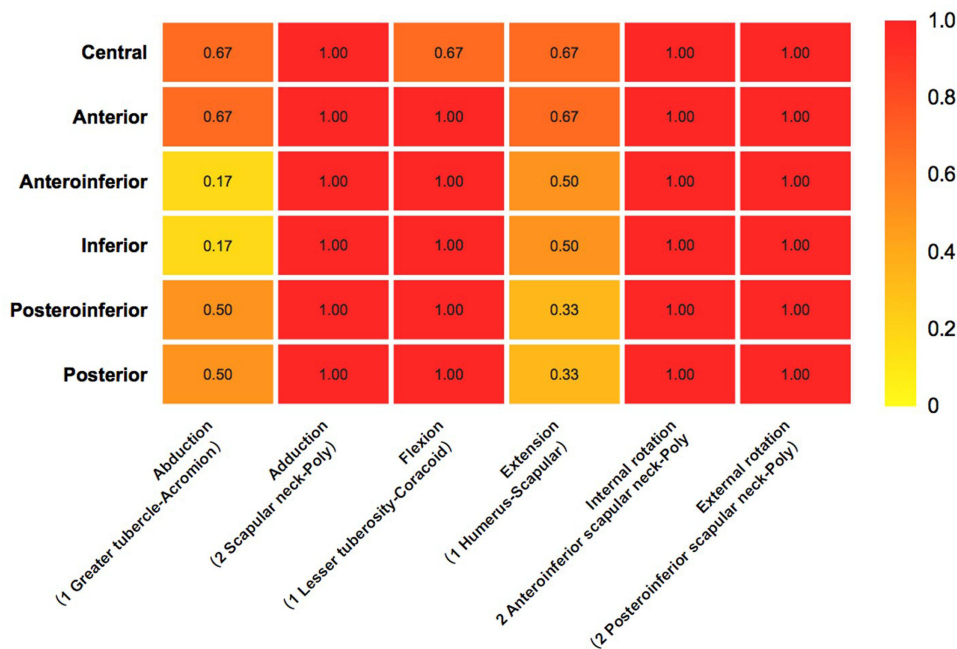


Figure 7 Graph presents a heatmap of the frequency of impingement locations for 6 different glenosphere eccentricities positions under different tilt and lateral offset combinations. Impingement type:1 represents impingement between bones and 2 represents impingement between bone and implant. In abduction, the frequency of impingement between the greater tuberosity and acromion; in adduction, the frequency of impingement between the scapular neck and poly; in flexion, the frequency of impingement between the lesser tuberosity and coracoid; in extension, the frequency of impingement between the humerus and scapular neck; in IR and ER, the frequency of impingement between the scapular neck and poly.

< 0.05). In addition, the anteroinferior eccentricity resulted in the greatest elongation in the deltoid (middle and posterior bundles) and the least shortening in the infraspinatus muscle. However, these differences were not statistically significant ( $p > 0.05$ ). Figure 8 illustrates the comparison of muscle lengths at the shoulder joint in T0L4 for different glenosphere eccentricities.



**Table 1** Impingement Sites for Different Glenoid Options When the Glensphere Anteroinferior Eccentricities

Glenoid Options	Abduction	Adduction	Flexion	Extension	Internal Rotation	External Rotation
T0; L0	2 Supraglenoid-Poly	2 Scapular neck-Poly	1 Lesser tuberosity-Coracoid	1 Humerus-Scapular	2 Anteroinferior scapular neck-Poly	2 Posteroinferior scapular neck-Poly
T10; L0	1 Greater tubercle-Acromion	2 Scapular neck-Poly	1 Lesser tuberosity-Coracoid	1 Humerus-Scapular	2 Anteroinferior scapular neck-Poly	2 Posteroinferior scapular neck-Poly
T20; L0	2 Supraglenoid-Poly	2 Scapular neck-Poly	1 Lesser tuberosity-Coracoid	2 Scapular neck-Poly	2 Anteroinferior scapular neck-Poly	2 Posteroinferior scapular neck-Poly
T0; L4	1 Greater tubercle-Acromion	2 Scapular neck-Poly	1 Lesser tuberosity-Coracoid	1 Humerus-Scapular	2 Anteroinferior scapular neck-Poly	2 Posteroinferior scapular neck-Poly
T10; L4	1 Greater tubercle-Acromion	2 Scapular neck-Poly	1 Lesser tuberosity-Coracoid	1 Humerus-Scapular	2 Anteroinferior scapular neck-Poly	2 Posteroinferior scapular neck-Poly
T20; L4	1 Greater tubercle-Coracoid	2 Scapular neck-Poly	1 Lesser tuberosity-Coracoid	1 Humerus-Acromion base	2 Anteroinferior scapular neck-Poly	2 Posteroinferior scapular neck-Poly

**Notes:** T, tilt; L, lateral offset; Impingement type: 1 represents impingement between bones and 2 represents impingement between bone and implant.

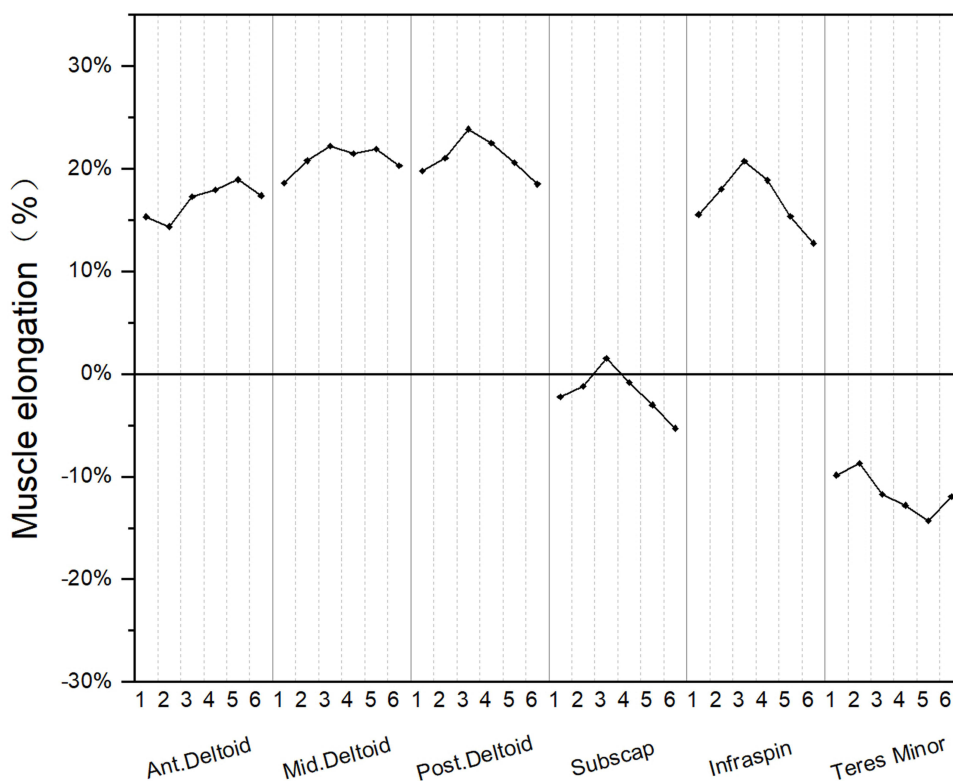


**Figure 8** This figure shows the effect of 6 different glenosphere eccentricities on the length changes of the anterior, middle, and posterior bundles of the deltoid muscle and the rotator cuff muscles in the TOL4 combination. 1, 2, 3, 4, 5, and 6 represent concentricity, inferior, posterior, anterior, anteroinferior, and posteroinferior glenosphere eccentricities, respectively. A positive percentage indicates elongation of the muscle relative to the normal shoulder, whereas a negative percentage indicates shortening of the muscle relative to the normal shoulder.

## Discussion

RSA has become a popular treatment for arthritic shoulders with irreparable rotator cuff tears due to its good clinical and biomechanical results.<sup>6,29</sup> However, the high complication rate associated with this procedure has generated controversy regarding its appropriate usage.<sup>30</sup> Modern glenoid components are still associated with impingement and notching, which can restrict ROM and potentially lead to glenoid loosening and component failure.<sup>31</sup> Therefore, many designs and techniques of RSA implants aim to optimize ROM while avoiding excessive muscle tension. To our knowledge, there is currently no comprehensive study that evaluates the effects of all six different offset positions on the free-impingement ROM, risk of impingement, and muscle length.

In this study, we constructed the three-dimensional CT-based computer shoulder joint model and performed surgical simulations of RSA with different glenosphere eccentricities according to surgical procedures. The standardized simulation of shoulder motion in different directions was used to analyze the bony impingement that limits abduction-adduction, flexion-extension, and rotation. The main findings of this study indicate that glenosphere eccentricity significantly affects flexion-extension, rotation, and global free-impingement ROM. Specifically, anteroinferior and inferior eccentricity demonstrated significant improvements in rotation and global ROM compared to concentricity.

## ROM

Among all 36 simulated combinations, only when the glenosphere concentricity at T20L0, the total global ROM did not exceed 50% of the native shoulder, and the others exceeded 50%. In both adduction and flexion movements, there are varying glenosphere eccentricities that do not reach 50% of the native shoulder. In all cases, the center is not achieved. This indicates that the utilized prosthetic design allows for a significant restoration of the native shoulder joint's ROM,<sup>32,33</sup> but the center performance is suboptimal during adduction and flexion activities.

In the abduction-adduction ROM, there were no significant differences among the different glenosphere eccentricities. However, anteroinferior eccentricity showed the maximum ROM in this plane, followed by inferior and concentricity. This trend is consistent with the findings of Arenas's study.<sup>32</sup> However, their research only focused on inferior, posteroinferior, and concentricity. Additionally, it alters the impingement site during abduction, leading to impingement between the polyethylene cup and the superior rim of the glenoid.

In the flexion-extension ROM, posteroinferior eccentricity showed the maximum ROM compared to other offsets. Specifically, in flexion, posteroinferior offset achieves the maximum ROM, showing significant advantages over concentricity, anterior, and anteroinferior eccentricities. This may be attributed to the fact that during flexion, the impingement sites for different eccentricities were consistent at the lesser tuberosity and the acromion. Posteroinferior eccentricity shifts the COR posteriorly and inferiorly, thereby increasing the ROM in flexion. However, the differences in various eccentricities during extension movements are not significant, possibly because extension inherently has a larger range of motion, and the offset distance is relatively smaller in comparison.

In the rotation, there were significant differences among the different glenosphere eccentricities. Anteroinferior and inferior eccentricity had advantages over concentricity and others. This finding is consistent with the standardized studies conducted by Arenas and Krämer.<sup>32,34</sup> Among the various glenosphere eccentricities, anteroinferior showed the maximum ROM in the rotation. We observed that the impingement sites remained consistent for both IR and ER, occurring between the polyethylene and the scapular neck. Therefore, we believe that these may increase the distance between the scapular neck and the polyethylene component, resulting in an increased ROM. Eric et al used planning software simulations and found that inferior eccentricity had a significant advantage over anterior eccentricity in ER activities.<sup>15</sup> This finding is consistent with our research results. Additionally, we also observed that posteroinferior eccentricity had a significant advantage over concentricity and anterior eccentricity. In IR, anteroinferior eccentricity demonstrated a significant advantage over concentricity. This indicates that inferior translation increases the ROM in rotation, while further anterior and posterior translation, respectively, increases the range of motion in internal and ER.

## Impingement

In this study, the impingement sites we observed were consistent with the locations and shapes of scapular and glenoid notches reported in previous cadaveric and radiographic research. We also observed that different glenosphere eccentricities resulted in different impingement sites. Additionally, we found that the tilt angle of the glenoid in anteroinferior eccentricity affected the type and sites of impingement during abduction and extension activities. This study provides valuable guidance and assistance in the prevention of impingement occurrences.

## Muscle Length

In the study of muscle length, only the subscapularis muscle was significantly affected by different glenosphere eccentricities. The anteroinferior eccentricity not only lengthened the subscapularis muscle and improved its function but also improved the ROM of IR and provided a greater contribution to IR. In this study, the infraspinatus muscle was found to be lengthened in all displacements, which is consistent with the findings of Alexandre et al.<sup>33,35</sup> However, this is inconsistent with the research conducted by Christopher et al, who found that the muscle was shortened.<sup>36</sup> This may be due to differences in the type and technique of prosthesis design used. In addition, we found that when the glenosphere anteroinferior eccentricity, the deltoid (middle and posterior bundles), infraspinatus, and teres minor muscles, which are external rotators, had the longest muscle lengths. This increased the wrapping of the deltoid and further improved the muscle function of abduction and ER. In addition, we also found that inferior tilt caused varying degrees of reduction in the increased lengths of the deltoid and rotator cuff muscles, while lateral offset caused a significant increase in these muscle lengths. This may be associated with the medialization and lateralization of the COR.

Utilizing these findings for preoperative planning and surgical techniques can help achieve constructs that are free impingement, and any limitations in ROM can be addressed through intraoperative soft-tissue releases. It is important to note that different glenosphere eccentricities contribute differently to shoulder function. Therefore, personalized adjustment of glenosphere eccentricity is necessary to achieve optimal functional outcomes.

## Limitation

This study also has some limitations: First, this study only assessed a 2mm eccentricity distance in different directions and did not evaluate the potential differences that larger eccentricity distances might bring. Second, this study primarily focused on assessing free-impingement rigid collisions and did not take into account the influence of soft tissue constraints, thus potentially deviating from the actual shoulder joint ROM. To better respond to physiologic shoulder motion after reverse shoulder surgery, we will utilize cadavers in future studies. Lastly, the extent of changes in the deltoid and rotator cuff muscles during motion and their impact on shoulder function were not specifically addressed.

## Conclusion

In conclusion, glenosphere eccentricity significantly affects rotation, total global ROM, and the length of the subscapularis muscle. Among them, anteroinferior offset achieved the maximum ROM in abduction-adduction, rotation, and total global activities. Both anteroinferior and inferior glenoid eccentricity showed significant advantages over the concentricity in total rotation and total global ROM. Additionally, anteroinferior eccentricity demonstrated advantages in IR ROM and IR muscle tension. However, there is no absolute advantage for a specific eccentricity position, and individual adjustments should be made based on the specific needs.

## Ethics Approval

This study was approved by the Ethics Committee of Beijing Chaoyang Hospital. Ethics Committee of Beijing Chaoyang Hospital waived the requirement for written informed consent because the study was retrospective, it did not have any adverse effect on patients' health, and it reported anonymized patient data. The authors announce that all methods were performed in accordance with the relevant guidelines and regulations. Strict confidentiality of patient data and adherence to the Declaration of Helsinki.

## Acknowledgments

I would like to appreciate my co-authors for their contributions to this study and the writing of this manuscript.

## Author Contributions

(I) Conception and design: X Xu; (II) Administrative support: J Zhou; (III) Provision of study materials or patients: X Xu; (IV) Collection and assembly of data: Q Sun, Y Liu; (V) Data analysis and interpretation: X Xu, Q Sun. All authors made a significant contribution to the work reported, whether that is in the conception, study design, execution, acquisition of data, analysis, and interpretation, or all these areas; took part in drafting, revising, or critically reviewing the article; gave final approval of the version to be published; have agreed on the journal to which the article has been submitted; and agree to be accountable for all aspects of the work.

## Funding

The correspondence author Junlin Zhou discloses receipt of the following financial support for the research, authorship, and publication of this article: National Natural Science Foundation of China (82272469), Beijing Key Clinical Specialty Project and Haidian Original Innovation Joint Fund of Beijing Natural Science Foundation (L212009).

## Disclosure

The authors declare that they have no conflicts of interest in this work.

## References

1. Boileau P, Watkinson DJ, Hatzidakis AM, Balg F. Grammont reverse prosthesis: design, rationale, and biomechanics. *J Shoulder Elbow Surg.* 2005;14(1 Suppl S):147S–161S. doi:10.1016/j.jse.2004.10.006
2. Longo UG, Papalia R, Castagna A, et al. Shoulder replacement: an epidemiological nationwide study from 2009 to 2019. *BMC Musculoskelet Disord.* 2022;23(1):889. doi:10.1186/s12891-022-05849-x

3. Best MJ, Aziz KT, Wilckens JH, McFarland EG, Srikanth U. Increasing incidence of primary reverse and anatomic total shoulder arthroplasty in the United States. *J Shoulder Elbow Surg.* 2021;30(5):1159–1166. doi:10.1016/j.jse.2020.08.010
4. Levy J, Frankle M, Mighell M, Pupello D. The use of the reverse shoulder prosthesis for the treatment of failed hemiarthroplasty for proximal humeral fracture. *J Bone Joint Surg Am.* 2007;89(2):292–300. doi:10.2106/00004623-200702000-00010
5. Palsis JA, Simpson KN, Matthews JH, Traven S, Eichinger JK, Friedman RJ. Current Trends in the Use of Shoulder Arthroplasty in the United States. *Orthopedics.* 2018;41(3):e416–e423. doi:10.3928/01477447-20180409-05
6. Boileau P, Watkinson D, Hatzidakis AM, Hovorka I, Neer Award 2005: the Grammont reverse shoulder prosthesis: results in cuff tear arthritis, fracture sequelae, and revision arthroplasty. *J Shoulder Elbow Surg.* 2006;15(5):527–540. doi:10.1016/j.jse.2006.01.003
7. Nam D, Kepler CK, Neviasser AS, et al. Reverse total shoulder arthroplasty: current concepts, results, and component wear analysis. *J Bone Joint Surg Am.* 2010;92 Suppl 2:23–35. doi:10.2106/JBJS.J.00769
8. Friedman RJ, Barcel DA, Eichinger JK. Scapular Notching in Reverse Total Shoulder Arthroplasty. *J Am Acad Orthop Surg.* 2019;27(6):200–209. doi:10.5435/JAAOS-D-17-00026
9. Nam D, Kepler CK, Nho SJ, Craig EV, Warren RF, Wright TM. Observations on retrieved humeral polyethylene components from reverse total shoulder arthroplasty. *J Shoulder Elbow Surg.* 2010;19(7):1003–1012. doi:10.1016/j.jse.2010.05.014
10. Kolmodin J, Davidson IU, Jun BJ, et al. Scapular Notching After Reverse Total Shoulder Arthroplasty: prediction Using Patient-Specific Osseous Anatomy, Implant Location, and Shoulder Motion. *J Bone Joint Surg Am.* 2018;100(13):1095–1103. doi:10.2106/JBJS.17.00242
11. Gutiérrez S, Comiskey CA 4th, Luo ZP, Pupello DR, Frankle MA. Range of impingement-free abduction and adduction deficit after reverse shoulder arthroplasty. Hierarchy of surgical and implant-design-related factors. *J Bone Joint Surg Am.* 2008;90(12):2606–2615. doi:10.2106/JBJS.H.00012
12. Collotte P, Erickson J, Vieira TD, Doms P, Walch G. Clinical and radiologic outcomes of eccentric glenosphere versus concentric glenosphere in reverse shoulder arthroplasty. *J Shoulder Elbow Surg.* 2021;30(8):1899–1906. doi:10.1016/j.jse.2020.10.032
13. Poon PC, Chou J, Young SW, Astley T. A comparison of concentric and eccentric glenospheres in reverse shoulder arthroplasty: a randomized controlled trial. *J Bone Joint Surg Am.* 2014;96(16):e138. doi:10.2106/JBJS.M.00941
14. De Biase CF, Ziveri G, Delcogliano M, et al. The use of an eccentric glenosphere compared with a concentric glenosphere in reverse total shoulder arthroplasty: two-year minimum follow-up results. *Int Orthop.* 2013;37(10):1949–1955. doi:10.1007/s00264-013-1947-9
15. Huish EG Jr, Athwal GS, Neyton L, Walch G. Adjusting Implant Size and Position Can Improve Internal Rotation After Reverse Total Shoulder Arthroplasty in a Three-dimensional Computational Model. *Clin Orthop Relat Res.* 2021;479(1):198–204. doi:10.1097/CORR.0000000000001526
16. Li X, Knutson Z, Choi D, et al. Effects of glenosphere positioning on impingement-free internal and external rotation after reverse total shoulder arthroplasty. *J Shoulder Elbow Surg.* 2013;22(6):807–813. doi:10.1016/j.jse.2012.07.013
17. Iliens J, Onsea J, Hoekstra H, Nijs S, Peetermans WE, Metsemakers WJ. Fracture-related infection in long bone fractures: a comprehensive analysis of the economic impact and influence on quality of life. *Injury.* 2021;52(11):3344–3349. doi:10.1016/j.injury.2021.08.023
18. Stall A, Paryavi E, Gupta R, Zadnik M, Hui E, O’Toole RV. Perioperative supplemental oxygen to reduce surgical site infection after open fixation of high-risk fractures: a randomized controlled pilot trial. *J Trauma Acute Care Surg.* 2013;75(4):657–663. doi:10.1097/TA.0b013e3182a1fe83
19. Paryavi E, Stall A, Gupta R, et al. Predictive model for surgical site infection risk after surgery for high-energy lower-extremity fractures: development of the risk of infection in orthopedic trauma surgery score. *J Trauma Acute Care Surg.* 2013;74(6):1521–1527. doi:10.1097/TA.0b013e318292158d
20. Akgün D, Wiethölter M, Siegert P, et al. The role of serum C-reactive protein in the diagnosis of periprosthetic shoulder infection. *Arch Orthop Trauma Surg.* 2022;142(8):1715–1721. doi:10.1007/s00402-021-03779-2
21. Gutiérrez S, Luo ZP, Levy J, Frankle MA. Arc of motion and socket depth in reverse shoulder implants. *Clin Biomech.* 2009;24(6):473–479. doi:10.1016/j.clinbiomech.2009.02.008
22. Knowles NK, Athwal GS, Keener JD, Ferreira LM. Regional bone density variations in osteoarthritic glenoids: a comparison of symmetric to asymmetric (type B2) erosion patterns. *J Shoulder Elbow Surg.* 2015;24(3):425–432. doi:10.1016/j.jse.2014.07.004
23. Wu G, van der Helm FC, Veeger HE, et al. ISB recommendation on definitions of joint coordinate systems of various joints for the reporting of human joint motion—Part II: shoulder, elbow, wrist and hand. *J Biomech.* 2005;38(5):981–992. doi:10.1016/j.jbiomech.2004.05.042
24. van Andel CJ, Wolterbeek N, Doorenbosch CA, Veeger DH, Harlaar J. Complete 3D kinematics of upper extremity functional tasks. *Gait Posture.* 2008;27(1):120–127. doi:10.1016/j.gaitpost.2007.03.002
25. Friedman RJ, Hawthorne KB, Genev BM. The use of computerized tomography in the measurement of glenoid version. *J Bone Joint Surg Am.* 1992;74(7):1032–1037. doi:10.2106/00004623-199274070-00009
26. Berhouet J, Garaud P, Favard L. Influence of glenoid component design and humeral component retroversion on internal and external rotation in reverse shoulder arthroplasty: a cadaver study. *Orthop Traumatol Surg Res.* 2013;99(8):887–894. doi:10.1016/j.otsr.2013.08.008
27. Gulotta LV, Choi D, Marinello P, et al. Humeral component retroversion in reverse total shoulder arthroplasty: a biomechanical study. *J Shoulder Elbow Surg.* 2012;21(9):1121–1127. doi:10.1016/j.jse.2011.07.027
28. Boileau P, Moineau G, Roussanne Y, O’Shea K. Bony increased-offset reversed shoulder arthroplasty: minimizing scapular impingement while maximizing glenoid fixation. *Clin Orthop Relat Res.* 2011;469(9):2558–2567. doi:10.1007/s11999-011-1775-4
29. Sirveaux F, Favard L, Oudet D, Huquet D, Walch G, Molé D. Grammont inverted total shoulder arthroplasty in the treatment of glenohumeral osteoarthritis with massive rupture of the cuff. Results of a multicenter study of 80 shoulders. *J Bone Joint Surg Br.* 2004;86(3):388–395. doi:10.1302/0301-620X.86B3.14024
30. Rockwood CA Jr. The reverse total shoulder prosthesis. The new kid on the block. *J Bone Joint Surg Am.* 2007;89(2):233–235. doi:10.2106/00004623-200702000-00001
31. Goetti P, Denard PJ, Collin P, Ibrahim M, Mazzolari A, Lädermann A. Biomechanics of anatomic and reverse shoulder arthroplasty. *EFORT Open Rev.* 2021;6(10):918–931. doi:10.1302/2058-5241.6.210014
32. Arenas-Miquelez A, Murphy RJ, Rosa A, Caironi D, Zumstein MA. Impact of humeral and glenoid component variations on range of motion in reverse geometry total shoulder arthroplasty: a standardized computer model study. *J Shoulder Elbow Surg.* 2021;30(4):763–771. doi:10.1016/j.jse.2020.07.026
33. Lädermann A, Denard PJ, Collin P, et al. Effect of humeral stem and glenosphere designs on range of motion and muscle length in reverse shoulder arthroplasty. *Int Orthop.* 2020;44(3):519–530. doi:10.1007/s00264-019-04463-2

34. Krämer M, Bäunker A, Wellmann M, Hurschler C, Smith T. Implant impingement during internal rotation after reverse shoulder arthroplasty. The effect of implant configuration and scapula anatomy: a biomechanical study. *Clin Biomech.* 2016;33:111–116. doi:10.1016/j.clinbiomech.2016.02.015
35. Lädermann A, Denard PJ, Boileau P, Farron A, Deransart P, Walch G. What is the best glenoid configuration in onlay reverse shoulder arthroplasty. *Int Orthop.* 2018;42(6):1339–1346. doi:10.1007/s00264-018-3850-x
36. Roche CP, Diep P, Hamilton M, et al. Impact of inferior glenoid tilt, humeral retroversion, bone grafting, and design parameters on muscle length and deltoid wrapping in reverse shoulder arthroplasty. *Bull Hosp Jt Dis.* 2013;71(4):284–293.

International Journal of General Medicine

Dovepress

## Publish your work in this journal

The International Journal of General Medicine is an international, peer-reviewed open-access journal that focuses on general and internal medicine, pathogenesis, epidemiology, diagnosis, monitoring and treatment protocols. The journal is characterized by the rapid reporting of reviews, original research and clinical studies across all disease areas. The manuscript management system is completely online and includes a very quick and fair peer-review system, which is all easy to use. Visit <http://www.dovepress.com/testimonials.php> to read real quotes from published authors.

Submit your manuscript here: <https://www.dovepress.com/international-journal-of-general-medicine-journal>